

Supplemental Document for TOG/SIGGRAPH Asia 2024 Paper “Large Scale Farm Scene Modeling from Remote Sensing Imagery”

ZHIQI XIAO and HAO JIANG*, Institute of Computing Technology, Chinese Academy of Sciences, University of Chinese Academy of Sciences, China

ZHIGANG DENG†, Department of Computer Science, University of Houston, USA

RAN LI, WENWEI HAN, and ZHAOQI WANG, Institute of Computing Technology, Chinese Academy of Sciences, University of Chinese Academy of Sciences, China

ACM Reference Format:

Zhiqi Xiao, Hao Jiang, Zhigang Deng, Ran Li, Wenwei Han, and Zhaoqi Wang. 2024. Supplemental Document for TOG/SIGGRAPH Asia 2024 Paper “Large Scale Farm Scene Modeling from Remote Sensing Imagery”. *ACM Trans. Graph.* 43, 6, Article 260 (December 2024), 31 pages. <https://doi.org/10.1145/3687918>

1 PLM PARAMETERS FOR ALL CATEGORIES

In Table 1, we list all the parameters for respective PLMs of fields, trees, and roads in our approach, and the ranges of these parameters.

2 ADDITIONAL EXPERIMENTAL RESULTS

In this section, we will show some additional experimental results. Due to the space limit, we cannot put those results in the main paper.

Table 1. Parameters for the respective PLMs of fields, trees, and roads

Parameters	Description	Range	
Field	δ	Crop type	[0-3]
	α	Angular offset	[0- $\pi/3$]
	r	Arc radius	[1-10]
	λ	Angular threshold	[0- $\pi/8$]
	ϵ	Curvature tolerance	[0-1]
	β	Deformation balance	[0-1]
	ω	Weight of energy function	[0-100]
	γ	Growth stage	[1-3]
	ν	Crop vitality	[0-1]
η	Crop placement jitter	[0-1]	
Tree	h	Planting space	[0.5-10]
	t	Total tree count	[0-1 × 10 ⁵]
	s	Average tree dimensions	[0.5-5]
	w	Weight of color cluster	[0-1]
Road	κ_x	X-coordinate	[0- X_{max}]
	κ_y	Y-coordinate	[0- Y_{max}]
	σ	Point type	[0-2]
	ϕ	Tangent direction	[0°, 360°]
	μ	Road width	[0-4]
	τ	Road type	[0-1]

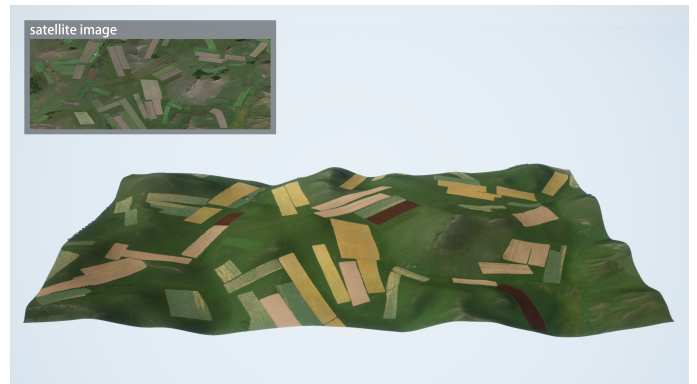


Fig. 1. An example of large-scale farm scenes modeled by our approach. The scene is composed of six satellite images stitched together. We employ the two-stage semantic segmentation process for each individual image, followed by alignment of the generated masks. Finally, we utilize appropriate PLMs to incorporate multi-scale details into each region.

* co-corresponding author

† co-corresponding author

Authors’ addresses: Zhiqi Xiao, xiaozhiqi22b@ict.ac.cn; Hao Jiang, jianghao@ict.ac.cn, Institute of Computing Technology, Chinese Academy of Sciences, and University of Chinese Academy of Sciences, China; Zhigang Deng, Department of Computer Science, University of Houston, USA, zdeng4@central.uh.edu; Ran Li, rleeiris@qq.com; Wenwei Han, asadirysue@gmail.com; Zhaoqi Wang, zqwang@ict.ac.cn, Institute of Computing Technology, Chinese Academy of Sciences, and University of Chinese Academy of Sciences, China.

Permission to make digital or hard copies of all or part of this work for personal or classroom use is granted without fee provided that copies are not made or distributed for profit or commercial advantage and that copies bear this notice and the full citation on the first page. Copyrights for components of this work owned by others than ACM must be honored. Abstracting with credit is permitted. To copy otherwise, or republish, to post on servers or to redistribute to lists, requires prior specific permission and/or a fee. Request permissions from permissions@acm.org.

© 2024 Association for Computing Machinery.

0730-0301/2024/12-ART260 \$15.00

<https://doi.org/10.1145/3687918>

2.1 The 1st Sugarcane Scene



Fig. 2. Satellite image of the 1st sugarcane scene.



Fig. 3. Rendered image of the 1st sugarcane scene (reconstructed by our method w/o Crop layout).



Fig. 4. Rendered image of the 1st sugarcane scene (reconstructed by our method w/o Crop vitality).



Fig. 5. Rendered image of the 1st sugarcane scene (reconstructed by our method w/o Tree).



Fig. 6. Rendered image of the 1st sugarcane scene reconstructed by our method (full version).



Fig. 7. Rendered close-up view of the 1st sugarcane scene reconstructed by our method (full version).

2.2 The 2nd Sugarcane Scene

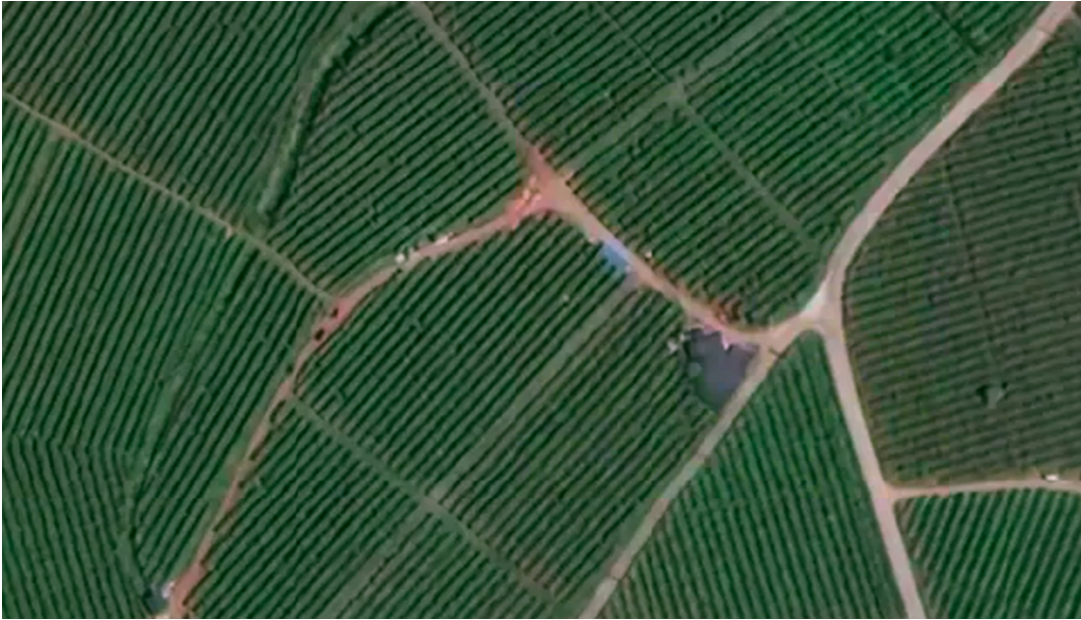


Fig. 8. Satellite image of the 2nd sugarcane scene.



Fig. 9. Rendered image of the 2nd sugarcane scene (reconstructed by our method w/o Crop layout).



Fig. 10. Rendered image of the 2nd sugarcane scene (reconstructed by our method w/o Crop vitality).



Fig. 11. Rendered image of the 2nd sugarcane scene (reconstructed by our method).



Fig. 12. Rendered close-up view of the 2nd sugarcane scene reconstructed by our method (full version).

2.3 The 3rd Sugarcane Scene



Fig. 13. Satellite image of the 3rd sugarcane scene.



Fig. 14. Rendered image of the 3rd sugarcane scene (reconstructed by our method w/o Crop layout).



Fig. 15. Rendered image of the 3rd sugarcane scene (reconstructed by our method w/o Crop vitality).



Fig. 16. Rendered image of the 3rd sugarcane scene (reconstructed by our method w/o Tree).



Fig. 17. Rendered image of the 3rd sugarcane scene (reconstructed by our method, full version).



Fig. 18. Rendered close-up view of the 3rd sugarcane scene reconstructed by our method (full version).

2.4 The 1st Harvested Land Scene



Fig. 19. Satellite image of the 1st harvested land scene.



Fig. 20. Rendered image of the 1st harvested land scene (reconstructed by our method).



Fig. 21. Rendered close-up view of the 1st harvested land scene (reconstructed by our method).

2.5 The 2nd Harvested Land Scene



Fig. 22. Satellite image of the 2nd harvested land scene.



Fig. 23. Rendered image of the 2nd harvested land scene (reconstructed by our method).



Fig. 24. Rendered close-up view of the 2nd harvested land scene (reconstructed by our method).

2.6 The 1st Wheat Scene



Fig. 25. Satellite image of the 1st wheat scene.



Fig. 26. Rendered image of the 1st wheat scene (reconstructed by our method w/o Crop layout).



Fig. 27. Rendered image of the 1t wheat scene (reconstructed by our method w/o Crop vitality).



Fig. 28. Rendered image of the 1st wheat scene (reconstructed by our method w/o Trees).



Fig. 29. Rendered image of the 1st wheat scene (reconstructed by our method).



Fig. 30. Rendered close-up view of the 1st wheat scene (reconstructed by our method).

2.7 The 2nd Wheat Scene



Fig. 31. Satellite image of the 2nd wheat scene.



Fig. 32. Rendered image of the 2nd wheat scene (reconstructed by our method w/o Crop layout).



Fig. 33. Rendered image of the 2nd wheat scene (reconstructed by our method w/o Crop vitality).



Fig. 34. Rendered image of the 2nd wheat scene (reconstructed by our method w/o Tree).



Fig. 35. Rendered image of the 2nd wheat scene (reconstructed by our method).



Fig. 36. Rendered close-up view of the 2nd wheat scene (reconstructed by our method).

2.8 The Corn Scene



Fig. 37. Satellite image of a corn scene.



Fig. 38. Rendered image of a corn scene (reconstructed by our method w/o Crop layout).



Fig. 39. Rendered image of a corn scene (reconstructed by our method w/o Crop vitality).



Fig. 40. Rendered image of a corn scene (reconstructed by our method w/o Tree).



Fig. 41. Rendered image of a corn scene reconstructed by our method (full version).



Fig. 42. Rendered close-up view of a corn scene by our method.

3 MODELING RESULTS FROM FIVE EXPERT USERS – CLOSE-UP VIEW COMPARISON OF TWO METHODS



(a)



(b)

(c)

Fig. 43. Rendered Close-Up View Comparison of Two Methods for Scene 1. (a) Satellite image of the scene. (b) Rendered bird-eye view and close-up view of the scene (reconstructed by our method); (c) Rendered bird-eye view and close-up view of the scene (modeled by the expert manual method).



(a)



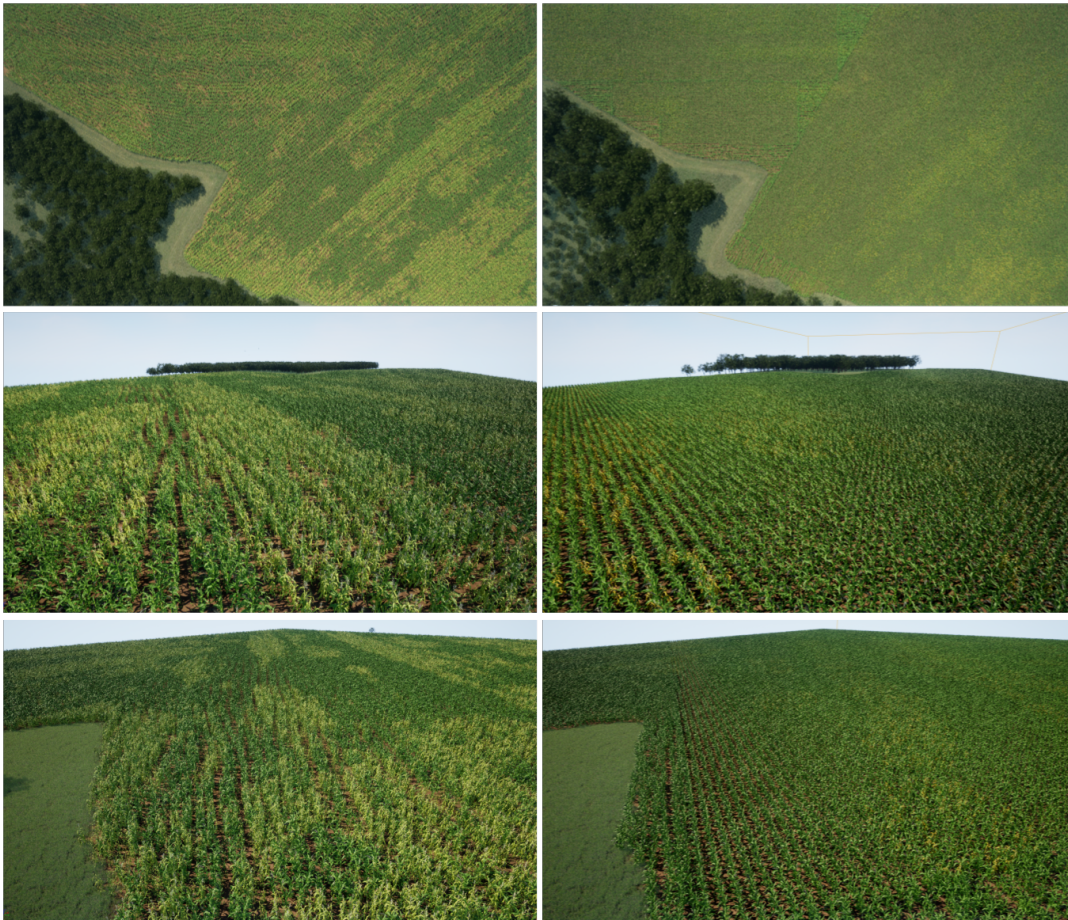
(b)

(c)

Fig. 44. Rendered Close-Up View Comparison of Two Methods for Scene 2. (a) Satellite image of the scene. (b) Rendered bird-eye view and close-up view of the scene (reconstructed by our method); (c) Rendered bird-eye view and close-up view of the scene (modeled by the expert manual method).



(a)



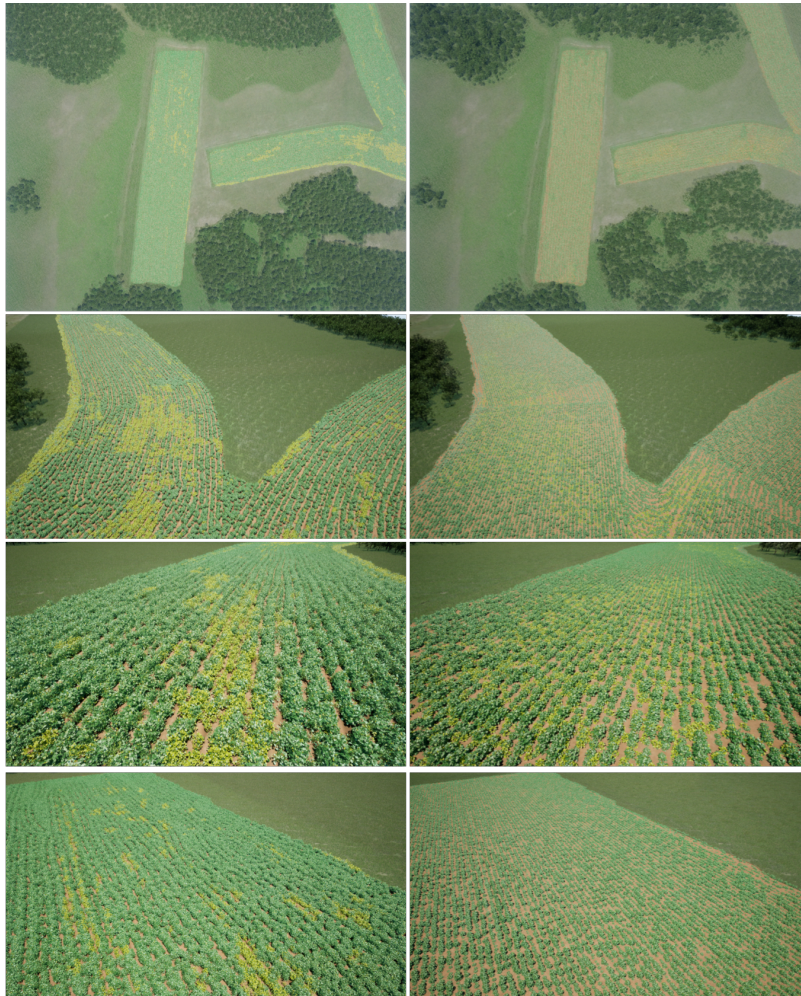
(b)

(c)

Fig. 45. Rendered Close-Up View Comparison of Two Methods for Scene 3. (a) Satellite image of the scene. (b) Rendered bird-eye view and close-up view of the scene (reconstructed by our method); (c) Rendered bird-eye view and close-up view of the scene (modeled by the expert manual method).



(a)



(b)

(c)

Fig. 46. Rendered Close-Up View Comparison of Two Methods for Scene 4. (a) Satellite image of the scene. (b) Rendered bird-eye view and close-up view of the scene (reconstructed by our method); (c) Rendered bird-eye view and close-up view of the scene (modeled by the expert manual method).



(a)



(b)

(c)

Fig. 47. Rendered Close-Up View Comparison of Two Methods for Scene 5. (a) Satellite image of the scene. (b) Rendered bird-eye view and close-up view of the scene (reconstructed by our method); (c) Rendered bird-eye view and close-up view of the scene (modeled by the expert manual method).

4 COTTON SCENE MODELING RESULTS.



Fig. 48. Satellite image of the scene of the cotton scene.



Fig. 49. Rendered close-up view of the cotton scene reconstructed by our method.



Fig. 50. Rendered close-up view of the cotton scene reconstructed by our method.



Fig. 51. Rendered close-up view of the cotton scene reconstructed by our method.



Fig. 52. Rendered close-up view of the cotton scene reconstructed by our method.